



NIH PUBLIC ACCESS

Author Manuscript

Arterioscler Thromb Vasc Biol. Author manuscript; available in PMC 2012 November 1.

Published in final edited form as:

Arterioscler Thromb Vasc Biol. 2011 November ; 31(11): 2509–2517. doi:10.1161/ATVBAHA.111.236828.

Human Thrombomodulin Knockin Mice Reveal Differential Effects of Human Thrombomodulin on Thrombosis and Atherosclerosis

Thomas J. Raife¹, Denis M. Dwyre¹, Jeff W. Stevens², Rochelle A. Erger³, Lorie Leo², Katina M. Wilson², Jose A. Fernández⁴, Jennifer Wilder⁵, Hyung-Suk Kim⁵, John H. Griffin⁴, Nobuyo Maeda⁵, and Steven R. Lentz^{2,3}

¹Department of Pathology, University of Iowa Carver College of Medicine, Iowa City, IA

²Department of Internal Medicine, University of Iowa Carver College of Medicine, Iowa City, IA

³Veterans Affairs Medical Center, Iowa City, IA

⁴Department of Molecular & Experimental Medicine, Scripps Research Institute, La Jolla, CA

⁵Department of Pathology, University of North Carolina, Chapel Hill, NC

Abstract

Objective—We sought to develop a murine model to examine the antithrombotic and antiinflammatory functions of human thrombomodulin *in vivo*.

Methods and Results—Knockin mice that express human thrombomodulin from the murine thrombomodulin gene locus were generated. Compared with wild-type mice, human thrombomodulin knockin mice exhibited decreased protein C activation in the aorta ($P < 0.01$) and lung ($P < 0.001$). Activation of endogenous protein C following infusion of thrombin was decreased by 90% in knockin mice compared with wild-type mice ($P < 0.05$). Carotid artery thrombosis induced by photochemical injury occurred more rapidly in knockin mice (12 ± 3 minutes) than wild-type mice (31 ± 6 minutes; $P < 0.05$). No differences in serum cytokine levels were detected between knockin and wild-type mice after injection of endotoxin. When crossed with apolipoprotein E-deficient mice and fed a Western diet, knockin mice had a further decrease in protein C activation but did not exhibit increased atherosclerosis.

Conclusion—Expression of human thrombomodulin in place of murine thrombomodulin produces viable mice with a prothrombotic phenotype but unaltered responses to systemic inflammatory or atherogenic stimuli. This “humanized” animal model will be useful for investigating the function of human thrombomodulin under pathophysiological conditions *in vivo*.

Keywords

thrombomodulin; protein C; inflammation; atherosclerosis; thrombosis

Thrombomodulin is an endothelial cell-surface thrombin receptor that modulates hemostasis and inflammation.^{1–3} When bound to thrombomodulin, thrombin efficiently catalyzes production of activated protein C (APC), a clinically important endogenous anticoagulant.

Address correspondence to: Steven R. Lentz, M.D., Ph.D., Department of Internal Medicine, C32 GH, The University of Iowa, Iowa City, IA 52242, Phone: 319-356-4048, Fax: 319-335-8848, steven-lentz@uiowa.edu.

Disclosures

SRL has served as a consultant for Novo Nordisk A/S and has an equity ownership interest in Celgene Corporation.

APC downregulates coagulation by proteolytically inactivating factors Va and VIIIa. In addition to its anticoagulant effects, APC inhibits endothelial inflammatory and cell death pathways⁴ through a mechanism that involves protease activated receptor-1 and the endothelial protein C receptor (EPCR).⁵⁻⁷ Thrombomodulin also modulates inflammation independently of APC, possibly by activating anti-inflammatory pathways through its N-terminal lectin domain,⁸⁻¹⁰ negatively regulating complement,¹¹ or by facilitating the activation of thrombin activatable fibrinolysis inhibitor, a procarboxypeptidase that may modulate both fibrinolysis and complement-mediated inflammation.²

Several murine models of altered thrombomodulin gene structure have been developed. Homozygous deletion of the murine thrombomodulin gene results in intrauterine lethality before E10.5.¹² The mechanism of embryonic death of thrombomodulin null embryos is related to thrombin-induced growth arrest of trophoblast cells.¹³ Embryonic development is not impaired in mice expressing thrombomodulin mutants with deletions of the C-terminal cytoplasmic or N-terminal lectin domains.^{8, 14} Embryonic development also occurs normally in mice with a thrombomodulin mutation (TM^{ΔPro}) that markedly reduces protein C activation and predisposes mice to thrombosis during hypoxia.¹⁵ This observation suggests that low levels of APC are sufficient for normal embryogenesis and placental development.

Because of interspecies differences in thrombomodulin structure and function, current murine models provide only limited insights into the pathophysiological role of human thrombomodulin *in vivo*. We therefore sought to develop knockin mice that express human thrombomodulin in the absence of murine thrombomodulin and to determine if such mice can be used to investigate the function of human thrombomodulin under pathophysiological conditions *in vivo*. Our results indicate that mice expressing human thrombomodulin from the murine thrombomodulin gene locus are partially protected from embryonic lethality and have normal post-natal development and survival. Compared with wild-type mice, human thrombomodulin knockin mice have a prothrombotic phenotype characterized by decreased protein C activation and enhanced susceptibility to experimental thrombosis but they do not exhibit impaired systemic anti-inflammatory responses or enhanced susceptibility to atherosclerosis. These findings reveal differential species-specific effects of murine and human thrombomodulin in regulating thrombosis vs. inflammation, and demonstrate that the human thrombomodulin knockin mouse is an instructive model for investigating the pathophysiological role of human thrombomodulin *in vivo*.

METHODS

Generation of human thrombomodulin knockin mice

Two separate lines of human thrombomodulin knockin mice, designated *Hn* and *Hthm*, were generated by targeted replacement of the murine thrombomodulin (*Thbd*) gene with the homologous gene segment containing the human thrombomodulin (*THBD*) coding sequence (see Supplemental Methods and Supplemental Figure I for details). Animal protocols were approved by the University of North Carolina or University of Iowa Animal Care and Use Committees.

Generation of *Apoe*^{-/-} *Hthm*/*Hthm* mice

Apolipoprotein E (*Apoe*) null mice¹⁶ on the C57BL/6 background were obtained from The Jackson Laboratory (Bar Harbor, ME) and crossbred with *Hthm*/⁺ mice for two generations to generate littermate *Apoe*^{-/-} mice that were either *Hthm*/*Hthm* or ^{+/+} at the thrombomodulin locus. Starting at three weeks of age, the mice were fed either a control diet (LM485, Harlan Teklad, Madison, WI) or high fat “Western” diet (TD003159, Harlan

Teklad) containing 20.3% fat. Experimental procedures were performed on male mice at 24 weeks of age. Blood from anesthetized mice was collected by cardiac puncture into EDTA (final concentration 5 mmol/L) and plasma cholesterol was measured using the Infinity Cholesterol Reagent kit (Thermo Electron Corporation; Louisville, CO).

Morphometric analysis of atherosclerotic lesions

Morphometric analyses of aortic sinus atherosclerotic lesion area was performed as described previously.¹⁷ Briefly, hearts embedded in paraffin were sectioned at 8 μ m serial intervals through the entire aortic sinus. The sections were stained with the Verhoeff - van Gieson method. Cross-sectional lesion area was calculated using the mean value of 5 sections, each 80 μ m apart, beginning at the aortic valve leaflets and spanning 320 μ m.

Measurement of thrombomodulin mRNA by quantitative PCR

Total RNA was isolated from lung, heart, or kidney of male mice using Trizol reagent. RNA was treated with DNase I to remove contaminating genomic DNA, and then reverse transcribed using Taqman reverse transcriptase reagents and random hexamer primers. Real-time PCR was performed using a 7700HT sequence detection system (Applied Biosystems) as described previously.¹⁸ Primers and probes were designed using Primer Express software (Applied Biosystems) to be specific for either murine *thbd* (forward, ATTTCCATTGCCAGCCTGTC; reverse, TGTACTCCAGCTCTGCACGA) or human *THBD* (forward, ATCTCCATCGCGAGCCTGTG; reverse, TGTACTCCATCTTGGCCCTG). A common probe (Fam-CGCCCTGCTTCTTGGCGCAGGT-Tamra) was used for both murine and human products. Total amounts of thrombomodulin transcripts in *Hthm/Hthm* and *+/+* mice were determined using a probe/primer set that detects regions common to the mouse and human transcripts (forward, GACAGCCCAGTTTCTTCCAA; reverse, TCTGGGATCTCCGCTGTATT; probe, Fam-CCACCTCCGCCAGTTGTCCAG-Tamra). Data were analyzed using the comparative threshold cycle ($\Delta\Delta C_T$) method,¹⁹ with β -actin as the comparator, using Sequence Detection software version 1.6.3 (Applied Biosystems).

Immunohistochemistry

Sections of formalin-fixed, paraffin-embedded lung or tail from adult mice were deparaffinized, and endogenous peroxidase activity quenched with hydrogen peroxide. Sections were blocked with Power Block (Biogenex, San Ramon, CA) and stained with a 1:50 dilution of mouse monoclonal anti-human thrombomodulin antibody (DakoCytomation, Carpinteria, CA) in PBS. LSAB II linker-horseradish peroxidase (DakoCytomation) was applied, and staining was visualized with diaminobenzidine (DakoCytomation). Sections were counterstained with Harris hematoxylin without acid.

Thrombomodulin antigen

Lung lysates were prepared by homogenization in 0.02 M Tris-HCl, 0.1 M NaCl, 2% Triton X-100 (pH 8.0) as described.²⁰ Human thrombomodulin antigen was measured by ELISA (Asserachrom Thrombomodulin, Diagnostica Stago, Franconville, France). To measure mouse thrombomodulin antigen, immunoassay plates (Nunc-Immuno plate, Polysorp surface, flat bottom, Nalge Nunc International, Rochester, NY) were coated overnight at 4°C with 1 μ g per well of polyclonal goat anti-mouse thrombomodulin (R&D Systems, Inc., Minneapolis, MN) in 20 mM carbonate (pH 9.2), 0.02% sodium azide. After washing 3 times, wells were blocked with 1% bovine serum albumin (Research Products International Corp, Prospect, IL) in 50 mM Tris-HCl (pH 7.4), 150 mM NaCl. Lung lysate samples (40 μ g protein per well) or recombinant mouse thrombomodulin (R&D Systems, Inc.) standard samples were added and incubated for one hour at room temperature followed by washing.

Monoclonal rat anti-mouse thrombomodulin (0.2 µg/well, R&D Systems, Inc.) was added and incubated for one hour at room temperature. After 3 additional washes, anti-rat IgG-alkaline phosphatase conjugate antibody (0.064 µg/well, Sigma-Aldrich, St. Louis, MO) was added and incubated for one hour at room temperature. After 3 additional washes, para-nitrophenol phosphate substrate (Sigma-Aldrich) was added and color development was monitored at 405 nm in a 96-well plate reader (Spectra Max 190, Molecular Devices, Woburn, MA). The standard curve was linear over a range of 0.1 to 2.0 nmol/L recombinant mouse thrombomodulin. No cross-reactivity with recombinant human thrombomodulin was detected at concentrations up to 4 nmol/L. The total protein concentration of lung lysates was measured using a modified Bradford assay (Bio-Rad Laboratories, Richmond, CA).

Protein C activation

Activation of exogenous protein C by thrombin was measured in freshly isolated rings of proximal aorta (1.0 mm in length), or in lung lysates, using a two-stage assay described previously.^{20, 21} Activation assays were performed using either 2.6 nM human thrombin and 150 nM human protein C²⁰ or 2.6 nM murine thrombin (Haematologic Technologies, Essex Junction, VT) and 150 nM murine protein C.²² Reference curves were generated using rabbit lung thrombomodulin (American Diagnostica, Stamford, CT). One unit of activity was defined as the amount of APC generated in the presence of 1.0 nmol/L rabbit thrombomodulin.

Activation of endogenous protein C was measured in response to infusion of human thrombin in adult mice. Mice anesthetized with sodium pentobarbital (70–90 mg/kg) were secured in a supine position under a dissecting microscope and ventilated mechanically with room air and supplemental oxygen as described previously.^{21, 23} A heating pad was used to maintain body temperature at 36–37°C. Human thrombin (Haematologic Technologies) (40 units/kg) or saline was rapidly infused into the right cardiac ventricle in a total volume of 100 µl. After 10 minutes, blood was collected by cardiac puncture into a 1/10th volume of 0.1 M sodium citrate containing 0.5 M benzamidine. The concentration of murine APC in citrate/benzamidine-treated plasma was measured as described previously²⁴ and reported as percent of APC in a pool of normal mouse plasma. For experiments performed with *ApoE*^{-/-} – *Hthm/Hthm* mice, murine APC was measured using an enzyme capture assay. Citrate-anticoagulated plasma samples containing 30 mM benzamidine were added to Nunc MaxiSorp plates (Fisher Scientific; Pittsburg PA) coated with 5 µg/ml anti-mouse APC (AMGDPC 1587), a generous gift from Charles Esmon (Oklahoma Medical Research Foundation, Oklahoma City, OK). The activity of bound APC was determined by incubation for 24 hours at 37°C with Spectrozyme PCa (American Diagnostica, Inc., Stamford, CT), followed by acid quenching and determination of absorbance using a microplate reader (Spectra Max 190; Molecular Devices; Sunnyvale, CA). Mouse APC (Haematological Technologies Inc., Essex Junction, VT) was used to standardize the assay.

Direct anticoagulant activity

To measure the direct anticoagulant activity of thrombomodulin, lung lysates were incubated with 1 nM human α -thrombin (HT3054, Enzyme Research, South Bend, IL) and bovine fibrinogen (1 mg/ml, Sigma, St. Louis, MO) and the time to clot formation was measured using a fibrometer (BBL FibroSystem, Becton Dickinson, Franklin Lakes, NJ).

Glycosaminoglycan hydrolysis

To determine the effect of glycosaminoglycan (GAG) on thrombomodulin activity, lung lysates were incubated for 16 hours at 37°C with or without chondroitin sulfate ABC lyase (Seikagaku America, Falmouth, MA) at 0.2 units/mg protein final concentration in 50 mM Tris-HCl containing 100 mM NaCl, 0.5 mM sodium acetate, leupeptin (20 µg/ml), pepstatin

(10 µg/ml), and 2.5 mM o-phenanthroline, pH 8.0. The reaction was stopped by incubating the solution at 90°C for 1 minute. To control for the efficiency of chondroitin sulfate lyase activity, a chondroitin sulfate-containing proteoglycan (aggrecan) from rat chondrosarcoma²⁵ was added to the chondroitin sulfate lyase-lung lysate mixtures. The mixtures were electrophoresed using 7.5% SDS-PAGE and stained with Coomassie blue to detect a characteristic 94 kDa aggrecan peptide devoid of GAG.²⁵ Protein C activation and direct anticoagulant activity assays were then performed using chondroitin sulfate lyase-treated or control lung lysates.

Carotid artery thrombosis

Carotid artery thrombosis was induced by photochemical injury as described.^{21, 23} Mice anesthetized with sodium pentobarbital (70–90 mg/kg) were ventilated mechanically with room air and supplemental oxygen. Blood flow in the right carotid artery was measured with a 0.5 PSB Doppler flow probe (Transonic Systems, Ithaca, NY). To induce endothelial injury, the right common carotid artery was transilluminated continuously with a 1.5-mV, 540 nm green laser (Melles Griot, Carlsbad, CA) from a distance of 6 cm, and rose bengal (25 to 50 mg/kg) was injected via a femoral vein catheter. Blood flow was monitored continuously for 90 minutes or until stable occlusion occurred. Stable occlusion was defined as the time at which blood flow remained absent for ≥ 10 minutes.

Response to endotoxin

Endotoxin (E. coli bacterial LPS serotype 055:B5) was purchased from Sigma-Aldrich, St. Louis, MO. Mice were injected intraperitoneally with 8 mg/kg LPS or saline in a volume of 100 µL. After 4 hours, serum was isolated for measurement of interleukin 6, interleukin 1β, and tumor necrosis factor-α by Quantikine immunoassay kits (R&D Systems, Inc. Minneapolis, MN). Plasma and serum were frozen at –80°C until assayed.

Statistical analyses

Comparisons between mouse genotypes were performed using the unpaired 2-tailed, Student's t-test or one-way ANOVA. Occlusion times were compared with the Mann-Whitney rank sum test. Viability data were analyzed using the chi-square test. Statistical significance was defined as a P value less than 0.05. Values are reported as mean ± SE. Except where indicated, all statistical comparisons were performed between littermates and all experimental groups included both female and male mice.

RESULTS

Generation and viability of human thrombomodulin knockin mice

Two separate lines of human thrombomodulin knockin mice, designated *Hn* and *Hthm*, were generated by targeted replacement of the murine *Thbd* gene with the homologous gene segment containing the human *THBD* coding sequence (Supplemental Figure I). The *Hn* line contained a loxP-flanked (floxed) neomycin resistance gene within the thrombomodulin 3' UTR. The *Hthm* line was generated by crossbreeding *Hn*/+ mice with transgenic mice expressing *Cre* recombinase²⁶ to excise the neomycin resistance gene.

In both the *Hn* and *Hthm* lines, the gross appearance of weaned heterozygous and homozygous human thrombomodulin knockin mice was normal, and no abnormalities in organ morphology or histology were observed. However, the number of viable homozygous *Hn/Hn* or *Hthm/Hthm* mice produced from heterozygous matings was decreased from expected Mendelian frequencies (Supplemental Tables I and II). Homozygous *Hn/Hn* mice represented only 5% of weaned offspring ($P < 0.05$ vs. the expected Mendelian frequency of 25%). The frequency of homozygous *Hthm/Hthm* offspring at weaning (14%) was greater

than for *Hn/Hn* homozygotes ($P < 0.001$), but was still less than the expected Mendelian frequency ($P < 0.05$). There were no significant differences in the frequencies of homozygous *Hthm/Hthm* or *Hn/Hn* offspring at weaning between mice on a 129/SvEv inbred background vs. mice on a mixed background of 129/SvEv and C57BL/6. *Hn/Hn* and *Hthm/Hthm* mice that survived weaning exhibited normal growth and survival. The mean weights of *Hn/Hn* and *Hthm/Hthm* mice between 12 and 18 months of age did not differ from *+/+* mice (data not shown).

Because mice with complete deficiency of thrombomodulin uniformly die before day 10 of embryogenesis,¹² we sought to determine if the decreased viability of human thrombomodulin knockin mice also was due to early embryonic lethality. The frequencies of *Hn/Hn* and *Hthm/Hthm* fetuses isolated from heterozygous matings on E10.5 were 16% and 23%, respectively (Supplemental Tables I and II), which suggests that early embryonic viability is relatively normal in human thrombomodulin knockin mice. On E17.5, the frequencies of *Hn/Hn* and *Hthm/Hthm* fetuses had decreased to 6% and 13%, respectively, quite similar to those observed at weaning. These findings suggest that homozygous replacement of the murine thrombomodulin allele with the *Hn* or *Hthm* alleles resulted in the partial loss of viability between E10.5 and E17.5. This effect on viability was more severe for *Hn/Hn* mice than for *Hthm/Hthm* mice.

Expression of thrombomodulin mRNA

Levels of total (murine plus human) thrombomodulin mRNA were measured in lung and heart isolated from adult *+/+*, *Hthm/Hthm*, and *Hn/Hn* mice using real-time PCR primers that detect both murine and human transcripts (Table 1). The levels of total thrombomodulin mRNA in the lung of *Hthm/Hthm* and *Hn/Hn* mice were not significantly different from those in *+/+* mice. In the heart, the levels of total thrombomodulin mRNA were similar in *+/+* and *Hthm/Hthm* mice, but were 50% lower in *Hn/Hn* mice than in *+/+* mice ($P < 0.05$).

Levels of individual murine thrombomodulin and human thrombomodulin transcripts were measured in *+/+*, *Hthm/+*, and *Hn/+* mice using species-specific real-time PCR primers (Table 2). Levels of murine thrombomodulin mRNA in the lung, heart, and kidney of *Hthm/+* mice were 50–60% lower than levels measured in *+/+* mice ($P < 0.05$). Levels of murine thrombomodulin mRNA in the lung, heart, and kidney of *Hn/+* mice were 40–65% lower than those in *+/+* mice ($P < 0.05$). These findings indicate that the presence of the targeted allele in heterozygous *Hthm/+* or *Hn/+* mice does not have a major influence on thrombomodulin expression from the wild-type allele. As expected, human thrombomodulin mRNA was not detected in *+/+* mice. The relative expression of human thrombomodulin mRNA in the lung and kidney was similar in *Hthm/+* and *Hn/+* mice. In the heart, there was a trend toward lower levels of human thrombomodulin mRNA in *Hn/+* mice compared with *Hthm/+* mice (8 ± 2 vs. $15 \pm 4\%$; $P = 0.24$), a finding that is consistent with the lower level of total thrombomodulin mRNA in the heart of *Hn/Hn* mice (Table 1).

Expression of human thrombomodulin protein

Expression of human thrombomodulin protein in *Hthm/+* and *Hthm/Hthm* mice was demonstrated by immunohistochemistry and ELISA (Figure 1). Immunohistochemical staining of tail cross-sections using a monoclonal anti-human thrombomodulin antibody was strongly positive in endothelium and keratinocytes in *Hthm/Hthm* mice, moderately positive in *Hthm/+* mice, and negative in *+/+* mice (Figure 1, A–C). This expression pattern is consistent with that observed previously for thrombomodulin in mice and humans.^{27, 28} Immunofluorescence staining of lung sections also revealed endothelium-specific staining for human thrombomodulin in *Hthm/+* and *Hthm/Hthm* mice, whereas staining for murine thrombomodulin was detected in *+/+* and *Hthm/+* mice (Supplemental Figure III). Co-

localization of murine and human thrombomodulin was observed in lung endothelium (Supplemental Figure IV).

Human thrombomodulin antigen levels measured by ELISA in lung lysates were concordant with immunohistochemical observations (Figure 1D). Human thrombomodulin antigen was approximately twice as high in *Hthm/Hthm* mice compared with *Hthm/+* mice ($P = 0.01$). Murine thrombomodulin antigen levels measured by ELISA in lung lysates were decreased by approximately 70% in *Hthm/+* mice compared with $+/+$ mice ($P < 0.01$) (Figure 1E).

Protein C activation

Activation of protein C in aortic rings and lung lysates was measured *in vitro* using human protein C and human thrombin. Generation of APC was similar in aortic rings from $+/+$ and *Hthm/+* mice (Figure 2A). APC generation was decreased by 28% in aortic rings from *Hn/+* mice ($P < 0.05$ vs. $+/+$ mice), and by approximately 60% in aortic rings from both *Hthm/Hthm* and *Hn/Hn* mice ($P < 0.01$ vs. $+/+$ mice). With lung lysates (Figure 2B), generation of APC was decreased by approximately 50% for *Hthm/+* and *Hn/+* mice ($P < 0.05$ vs. $+/+$ mice), 75% for *Hthm/Hthm* mice ($P < 0.001$ vs. $+/+$ mice), and 90% for *Hn/Hn* mice ($P < 0.05$ vs. $+/+$ mice). To determine if differences in protein C activation also occurred with murine reagents, activation of murine protein C was measured with lung lysates from $+/+$, *Hthm/+*, and *Hthm/Hthm* mice using murine thrombin. Compared with lysates from $+/+$ mice, lysates from *Hthm/+* mice generated 52% less APC ($P < 0.05$) and lysates from *Hthm/Hthm* mice generated 86% less APC ($P < 0.001$) (Figure 2C).

Activation of endogenous murine protein C *in vivo* was assessed by measuring plasma levels of APC in $+/+$, *Hthm/+*, and *Hthm/Hthm* mice following infusion of saline vehicle or 40 U/kg human thrombin (Figure 2D). Compared with infusion of saline, infusion of thrombin produced a 2.7-fold increase in plasma APC concentration in $+/+$ mice ($P < 0.05$) but no significant increase in *Hthm/+* or *Hthm/Hthm* mice.

Effect of glycosaminoglycan hydrolysis on thrombomodulin activity

To determine if the decreased thrombomodulin activity of human thrombomodulin knockin mice was caused by differential effects of GAG attachment to thrombomodulin, lung lysates from $+/+$ or *Hthm/Hthm* mice were incubated with chondroitin sulfate ABC lyase prior to performing protein C activation or direct anticoagulant activity assays. The protein C activation activity of thrombomodulin in lung lysates from $+/+$ or *Hthm/Hthm* mice was not significantly affected by treatment with chondroitin sulfate lyase (Supplemental Figure VA). In contrast, the direct anticoagulant activity of thrombomodulin (i.e. the ability of thrombomodulin to directly inhibit the fibrinogen cleaving activity of thrombin), which is highly sensitive to its GAG content,²⁹ was decreased by approximately 40% after GAG hydrolysis in both the $+/+$ and *Hthm/Hthm* samples (Supplemental Figure VB). These results suggested that GAG attachment contributes equivalently to the direct anticoagulant activity of murine and human thrombomodulin expressed in mouse lung.

Carotid artery thrombosis

The time to thrombotic occlusion of the carotid artery after photochemical injury was measured in $+/+$, *Hthm/+*, and *Hthm/Hthm* mice (Figure 3). Occlusion times did not differ between $+/+$ and *Hthm/+* mice, but the mean time to stable occlusion was decreased by more than 60% in *Hthm/Hthm* mice (12 ± 3 minutes) compared with $+/+$ mice (31 ± 6 minutes) ($P < 0.05$).

Response to endotoxin

The inflammatory response to intraperitoneal injection of a sublethal dose of 8 mg/kg *E. coli* LPS was determined by measurement of serum cytokine levels in *+/+* and *Hthm/Hthm* mice 4 hours after LPS administration. Serum levels of IL-6 (Figure 4A), IL-1 β (Figure 4B), and TNF α (Figure 4C) all increased significantly and equivalently after LPS administration in *+/+* and *Hthm/Hthm* mice ($P < 0.05$ vs. saline).

Phenotype of *Apoe*^{-/-} *Hthm/Hthm* mice

To determine the effects of hypercholesterolemia in human thrombomodulin knockin mice, *Apoe*^{-/-} mice were crossbred with *Hthm*^{+/+} mice for two generations to generate littermate *Apoe*^{-/-} mice that were either *Hthm/Hthm* or *+/+* at the thrombomodulin locus. Starting at three weeks of age, male mice were fed either a control diet or high fat “Western” diet until they were studied at 24 weeks of age. Compared with the control diet, the high fat diet produced a similar 2-fold increase in plasma total cholesterol levels in *Apoe*^{-/-} and *Apoe*^{-/-} *Hthm/Hthm* mice ($P < 0.01$) (Figure 5A). The high fat diet also produced similar increases in cross-sectional atherosclerotic lesion area, measured in the aortic sinus, compared with the control diet in *Apoe*^{-/-} and *Apoe*^{-/-} *Hthm/Hthm* mice ($P < 0.01$) (Figure 5B). Following infusion of thrombin, circulating plasma levels of APC were significantly lower in *Apoe*^{-/-} *Hthm/Hthm* mice compared with littermate *Apoe*^{-/-} mice fed either the control or high fat diets ($P < 0.01$) (Figure 5C). Notably, the amount of circulating APC generated in *Apoe*^{-/-} *Hthm/Hthm* mice was significantly lower with the high fat diet than the control diet ($P < 0.05$). Finally, the time to stable thrombotic occlusion of the carotid artery after photochemical injury was decreased markedly in *Apoe*^{-/-} or *Apoe*^{-/-} *Hthm/Hthm* mice fed the high fat diet ($P < 0.05$) (Figure 5D), confirming that hypercholesterolemia induces a prothrombotic phenotype in mice expressing either murine or human thrombomodulin.

DISCUSSION

We generated knockin mice that express human thrombomodulin in the absence of murine thrombomodulin. Human thrombomodulin knockin mice exhibited a prothrombotic phenotype, with decreased activation of protein C *in vivo* following thrombin infusion and an accelerated thrombotic response to carotid artery injury. Interestingly, exposure to endotoxin produced identical systemic cytokine responses in wild-type and human thrombomodulin knockin mice, which suggests that despite their markedly different anticoagulant profiles, mice expressing murine and human thrombomodulin have similar inflammatory responses *in vivo*. Mice expressing human or murine thrombomodulin also had similar susceptibilities to atherosclerosis when crossed to an apolipoprotein E-deficient background. Interestingly, hypercholesterolemia produced a significant impairment of protein C activation in mice expressing human thrombomodulin, which demonstrates the potential utility of the human thrombomodulin knockin mouse as a pathophysiological model for the study of human thrombomodulin function in conditions such as atherosclerosis.

Expression of human thrombomodulin in place of murine thrombomodulin partially bypassed the uniform embryonic lethality that occurs with complete deficiency of murine thrombomodulin.¹² Approximately 50% of mice homozygous for the *Hthm* allele and 80% of mice homozygous for the *Hn* allele died between E10.5 and E17.5 (Supplemental Table I). Thrombomodulin is expressed in both trophoblasts and developing endothelium early in embryogenesis.¹ The mechanism of early embryonic death of thrombomodulin null embryos appears to be caused by growth arrest of trophoblast cells.¹³ Reconstitution of murine thrombomodulin expression in placental tissue rescues thrombomodulin null embryos from early embryonic lethality, and reveals a secondary developmental block between days 12.5

and 16.5 that is caused by lack of thrombomodulin expression in endothelium.^{13, 30} Our findings suggest that human thrombomodulin can functionally substitute for murine thrombomodulin to bypass the early trophoblast-dependent developmental block, but only partially bypass the later, endothelium-dependent developmental block. The more severe embryonic loss in *Hn/Hn* mice compared with *Hthm/Hthm* mice may be due to slightly lower expression of human thrombomodulin in some tissues (Table 1), likely caused by the presence of the neomycin resistance gene within the 3'UTR of the *Hn* allele.

Compared with wild-type mice, human thrombomodulin knockin mice were hypomorphic for thrombomodulin activity and exhibited a prothrombotic phenotype, with a 50% shortening in the time to carotid artery occlusion following photochemical injury. The prothrombotic phenotype of human thrombomodulin knockin mice contrasts with the antithrombotic phenotype of human thrombomodulin transgenic mice reported recently by Crikis et al.³¹ An important distinction between these models is that the transgenic mouse model described by Crikis et al. is a thrombomodulin overexpression model in which the human thrombomodulin transgene is expressed in addition to endogenous murine thrombomodulin. Overexpression of (human + murine) thrombomodulin in these mice results in increased APC generation and protection from thrombosis.³¹ In contrast, the human thrombomodulin knockin mouse model reported here is a hypomorphic model in which human thrombomodulin is expressed instead of murine thrombomodulin. Compared with *+/+* mice, *Hthm/Hthm* mice had similar levels of thrombomodulin mRNA expression (Table 1) and higher levels of thrombomodulin antigen in the lung (Figure 1). These findings suggest that the prothrombotic phenotype (decreased protein C activation and enhanced susceptibility to arterial thrombosis) in *Hthm/Hthm* mice is unlikely to be caused by an alteration in thrombomodulin expression. Instead, the findings suggest that human thrombomodulin may be a less active anticoagulant than murine thrombomodulin *in vivo*.

We explored the possibility that differences in protein C activation between wild-type and human thrombomodulin knockin mice may be related to differences in modification by O-linked chondroitin sulfate GAG chains. Thrombomodulin's GAG chains provide secondary thrombin binding sites and enhance its anticoagulant function.^{32, 33} Both murine and human thrombomodulin contain GAG attachment consensus sequences within their serine/threonine rich domains.³⁴ In human thrombomodulin, the primary GAG attachment site is serine 474.³⁵ Mouse thrombomodulin has a homologous serine attachment site, but the flanking sequence contains a series of three acidic residues that may enhance the efficiency of GAG attachment.³⁶ Despite these sequence differences, when human and murine thrombomodulin were treated with chondroitin sulfate ABC lyase to remove GAG, no significant effects on protein C activation were observed (Supplemental Figure V). The direct anticoagulant function of both murine and human thrombomodulin was decreased by GAG removal, but the effects were similar for *+/+* and *Hthm/Hthm* mice. These results indicate that GAG attachment plays an equivalent role in the anticoagulant activity of murine and human thrombomodulin and suggest that the prothrombotic phenotype of human thrombomodulin knockin mice is not due to differential effects of GAG. It is more likely, therefore, that structural changes due to amino acid differences are responsible for the more potent antithrombotic activity of murine compared with human thrombomodulin.

It is possible but unlikely that the decreased protein C activation in human thrombomodulin knockin mice is related to the presence of the A455V polymorphism within the 6th EGF domain. This common human thrombomodulin polymorphism has been found to be associated with arterial thrombosis in some studies, but several large population studies have failed to confirm this association.^{37, 38} Several other candidate prothrombotic thrombomodulin mutations have been identified in human subjects with venous or arterial thrombosis, but the clinical significance of these gene variants remains uncertain.³⁷⁻³⁹

Mutations that impair the function of thrombomodulin were recently described in some patients with atypical hemolytic uremic syndrome.⁴⁰ The thrombomodulin knockin approach described in this study could potentially be utilized to directly examine the pathophysiological consequences of these and other human thrombomodulin gene variants.

Despite considerable progress in defining the role of thrombomodulin and the protein C activation pathway in susceptibility to thrombosis and modulation of inflammatory responses, the impact of this anticoagulant pathway on atherosclerosis is less well understood.⁴¹ Eitzman et al. observed accelerated atherogenesis in *ApoE*^{-/-} mice expressing the murine equivalent of the human factor V Leiden mutation, which confers resistance to APC.⁴² Seehaus et al. found that expression of a hypomorphic murine thrombomodulin mutation (TM^{ΔPro}) in *ApoE*^{-/-} mice had paradoxical effects on atherosclerosis; the atherosclerotic lesions were larger but also had histological features suggestive of enhanced plaque stability.⁴³ These observations raise the question of whether human thrombomodulin confers protection or susceptibility to atherosclerosis. Our findings indicate that mice expressing human or murine thrombomodulin have similar susceptibilities to atherosclerosis when crossed to the *ApoE*^{-/-} background despite their differing anticoagulant activities. The contrasting effects on atherosclerosis of the murine TM^{ΔPro} mutant studied by Seehaus et al. and human thrombomodulin in our study could be due to a relatively lower anticoagulant activity of the TM^{ΔPro} mutant.¹⁵ Alternatively, these findings might suggest that human thrombomodulin has protective effects on atherosclerosis that are independent of its anticoagulant activity. In either case, our results suggest that the human thrombomodulin knockin mouse may be an informative *in vivo* model for future studies investigating the role of human thrombomodulin in atherosclerosis and other pathophysiological conditions.

A limitation of many mouse models is that there often are species-specific functional differences between human and murine proteins that may alter responses to pathophysiological conditions or pharmacological interventions. The generation of human thrombomodulin knockin mice is a step toward humanizing the entire protein C system in mice. Such humanization might facilitate the discovery of small molecules that modify the human anticoagulant system and to study *in vivo* consequences of such modifications. The current model is limited because only the thrombomodulin gene locus was humanized and it is not possible to directly compare the functional activities of human versus murine thrombomodulin because of differences in their expression levels. Nevertheless, the availability of this model, as well as other similar models such as the humanized tissue factor mouse⁴⁴ may enhance the clinical relevance of mouse models of human thrombotic disease.

Supplementary Material

Refer to Web version on PubMed Central for supplementary material.

Acknowledgments

We thank the Core Pathology Research and the Central Microscopy Research Facilities of the University of Iowa for performance of immunohistochemistry and immunofluorescence.

Sources of Funding

Supported by the Office of Research and Development, Department of Veterans Affairs (SRL) and National Institutes of Health grants HL63943, NS24621, and HL62984 (SRL), T32 HL07344 (DMD), HL31950 (JHG), and HL42630 (NM).

References

1. Weiler H, Isermann BH. Thrombomodulin. *J Thromb Haemost*. 2003; 1:1515–1524. [PubMed: 12871287]
2. Van de Wouwer M, Collen D, Conway EM. Thrombomodulin-protein C-EPCR system: integrated to regulate coagulation and inflammation. *Arterioscler Thromb Vasc Biol*. 2004; 24:1374–1383. [PubMed: 15178554]
3. Esmon CT. Interactions between the innate immune and blood coagulation systems. *Trends Immunol*. 2004; 25:536–542. [PubMed: 15364056]
4. Joyce DE, Gelbert L, Ciaccia A, DeHoff B, Grinnell BW. Gene expression profile of antithrombotic protein C defines new mechanisms modulating inflammation and apoptosis. *J Biol Chem*. 2001; 276:11199–11203. [PubMed: 11278252]
5. Riewald M, Petrovan RJ, Donner A, Mueller BM, Ruf W. Activation of endothelial cell protease activated receptor 1 by the protein C pathway. *Science*. 2002; 296:1880–1882. [PubMed: 12052963]
6. Cheng T, Liu D, Griffin JH, Fernandez JA, Castellino F, Rosen ED, Fukudome K, Zlokovic BV. Activated protein C blocks p53-mediated apoptosis in ischemic human brain endothelium and is neuroprotective. *Nat Med*. 2003; 9:338–342. [PubMed: 12563316]
7. Mosnier LO, Griffin JH. Inhibition of staurosporine-induced apoptosis of endothelial cells by activated protein C requires protease-activated receptor-1 and endothelial cell protein C receptor. *Biochem J*. 2003; 373:65–70. [PubMed: 12683950]
8. Conway EM, Van de WM, Pollefeyt S, Jurk K, Van Aken H, De Vriese A, Weitz JI, Weiler H, Hellings PW, Schaeffer P, Herbert JM, Collen D, Theilmeier G. The lectin-like domain of thrombomodulin confers protection from neutrophil-mediated tissue damage by suppressing adhesion molecule expression via nuclear factor kappaB and mitogen-activated protein kinase pathways. *J Exp Med*. 2002; 196:565–577. [PubMed: 12208873]
9. Abeyama K, Stern DM, Ito Y, Kawahara K, Yoshimoto Y, Tanaka M, Uchimura T, Ida N, Yamazaki Y, Yamada S, Yamamoto Y, Yamamoto H, Iino S, Taniguchi N, Maruyama I. The N-terminal domain of thrombomodulin sequesters high-mobility group-B1 protein, a novel antiinflammatory mechanism. *J Clin Invest*. 2005; 115:1267–1274. [PubMed: 15841214]
10. Shi CS, Shi GY, Hsiao SM, Kao YC, Kuo KL, Ma CY, Kuo CH, Chang BI, Chang CF, Lin CH, Wong CH, Wu HL. Lectin-like domain of thrombomodulin binds to its specific ligand Lewis Y antigen and neutralizes lipopolysaccharide-induced inflammatory response. *Blood*. 2008; 112:3661–3670. [PubMed: 18711002]
11. Van de Wouwer M, Plaisance S, De VA, Waelkens E, Collen D, Persson J, Daha MR, Conway EM. The lectin-like domain of thrombomodulin interferes with complement activation and protects against arthritis. *J Thromb Haemost*. 2006; 4:1813–1824. [PubMed: 16879225]
12. Healy AM, Rayburn HB, Rosenberg RD, Weiler H. Absence of the blood-clotting regulator thrombomodulin causes embryonic lethality in mice before development of a functional cardiovascular system. *Proc Natl Acad Sci USA*. 1995; 92:850–854. [PubMed: 7846065]
13. Isermann B, Sood R, Pawlinski R, Zogg M, Kalloway S, Degen JL, Mackman N, Weiler H. The thrombomodulin-protein C system is essential for the maintenance of pregnancy. *Nat Med*. 2003; 9:331–337. [PubMed: 12579195]
14. Conway EM, Pollefeyt S, Cornelissen J, DeBaere I, Steiner-Mosonyi M, Weitz JI, Weiler-Guettler H, Carmeliet P, Collen D. Structure-function analyses of thrombomodulin by gene-targeting in mice: The cytoplasmic domain is not required for normal fetal development. *Blood*. 1999; 93:3442–3450. [PubMed: 10233896]
15. Weiler-Guettler H, Christie PD, Beeler DL, Healy AM, Hancock WW, Rayburn H, Edelberg JM, Rosenberg RD. A targeted point mutation in thrombomodulin generates viable mice with a prethrombotic state. *J Clin Invest*. 1998; 101:1983–1991. [PubMed: 9576763]
16. Zhang SH, Reddick RL, Piedrahita JA, Maeda N. Spontaneous hypercholesterolemia and arterial lesions in mice lacking apolipoprotein E. *Science*. 1992; 258:468–471. [PubMed: 1411543]

17. Wilson KM, McCaw RB, Leo L, Arning E, Lhotak S, Bottiglieri T, Austin RC, Lentz SR. Prothrombotic effects of hyperhomocysteinemia and hypercholesterolemia in ApoE-deficient mice. *Arterioscler Thromb Vasc Biol.* 2007; 27:233–240. [PubMed: 17082485]
18. Kim HS, Lee G, John SW, Maeda N, Smithies O. Molecular phenotyping for analyzing subtle genetic effects in mice: application to an angiotensinogen gene titration. *Proc Natl Acad Sci USA.* 2002; 99:4602–4607. [PubMed: 11904385]
19. Livak KJ, Schmittgen TD. Analysis of relative gene expression data using real-time quantitative PCR and the 2⁻(Delta Delta C(T)) Method. *Methods.* 2001; 25:402–408. [PubMed: 11846609]
20. Dayal S, Bottiglieri T, Arning E, Maeda N, Malinow MR, Sigmund CD, Heistad DD, Faraci FM, Lentz SR. Endothelial dysfunction and elevation of S-adenosylhomocysteine in cystathionine β -synthase-deficient mice. *Circ Res.* 2001; 88:1203–1209. [PubMed: 11397788]
21. Dayal S, Wilson KM, Leo L, Arning E, Bottiglieri T, Lentz SR. Enhanced susceptibility to arterial thrombosis in a murine model of hyperhomocysteinemia. *Blood.* 2006; 108:2237–2243. [PubMed: 16804115]
22. Fernandez JA, Xu X, Liu D, Zlokovic BV, Griffin JH. Recombinant murine-activated protein C is neuroprotective in a murine ischemic stroke model. *Blood Cells Mol Dis.* 2003; 30:271–276. [PubMed: 12737945]
23. Wilson KM, Lynch CM, Faraci FM, Lentz SR. Effect of mechanical ventilation on carotid artery thrombosis induced by photochemical injury in mice. *J Thromb Haemost.* 2003; 1:2669–2674. [PubMed: 14675104]
24. Fernandez JA, Lentz SR, Dwyre DM, Griffin JH. A novel ELISA for mouse activated protein C in plasma. *J Immunol Methods.* 2006; 314:174–181. [PubMed: 16828789]
25. Stevens JW, Oike Y, Handley C, Hascall VC, Hampton A, Catterson B. Characteristics of the core protein of the aggregating proteoglycan from the Swarm rat chondrosarcoma. *J Cell Biochem.* 1984; 26:247–259. [PubMed: 6530406]
26. Lakso M, Pichel JG, Gorman JR, Sauer B, Okamoto Y, Lee E, Alt FW, Westphal H. Efficient in vivo manipulation of mouse genomic sequences at the zygote stage. *Proc Natl Acad Sci USA.* 1996; 93:5860–5865. [PubMed: 8650183]
27. Raife TJ, Lager DJ, Peterson JJ, Erger RA, Lentz SR. Keratinocyte-specific expression of human thrombomodulin in transgenic mice: effects on epidermal differentiation and cutaneous wound healing. *J Invest Med.* 1998; 46:127–133.
28. Faust SN, Levin M, Harrison OB, Goldin RD, Lockhart MS, Kondaveeti S, Laszik Z, Esmon CT, Heyderman RS. Dysfunction of endothelial protein C activation in severe meningococcal sepsis. *N Eng J Med.* 2001; 345:408–416.
29. Sadler JE, Lentz SR, Sheehan JP, Tsiang M, Wu Q. Structure-function relationships of the thrombin-thrombomodulin interaction. *Haemostasis.* 1993; 23(suppl 1):183–193. [PubMed: 8388351]
30. Isermann B, Hendrickson SB, Hutley K, Wing M, Weiler H. Tissue-restricted expression of thrombomodulin in the placenta rescues thrombomodulin-deficient mice from early lethality and reveals a secondary developmental block. *Development.* 2001; 128:827–838. [PubMed: 11222138]
31. Crikis S, Zhang XM, Dezfouli S, Dwyer KM, Murray-Segal LM, Salvaris E, Selan C, Robson SC, Nandurkar HH, Cowan PJ, d'Apice AJ. Antiinflammatory and anticoagulant effects of transgenic expression of human thrombomodulin in mice. *Am J Transplant.* 2010
32. Ye J, Esmon CT, Johnson AE. The chondroitin sulfate moiety of thrombomodulin binds a second molecule of thrombin. *J Biol Chem.* 1993; 268:2373–2379. [PubMed: 8381406]
33. Lin JH, McLean K, Morser J, Young TA, Wydro RM, Andrews WH, Light DR. Modulation of glycosaminoglycan addition in naturally expressed and recombinant human thrombomodulin. *J Biol Chem.* 1994; 269:25021–25030. [PubMed: 7929188]
34. Dittman WA, Majerus PW. Structure and function of thrombomodulin: a natural anticoagulant. *Blood.* 1990; 75:329–336. [PubMed: 2153035]
35. Gerlitz B, Hassell T, Vlahos CJ, Parkinson JF, Bang NU, Grinnell BW. Identification of the predominant glycosaminoglycan-attachment site in soluble recombinant human thrombomodulin -

- potential regulation of functionality by glycosyltransferase competition for serine(474). *Biochem J.* 1993; 295:131–140. [PubMed: 8216207]
36. Esko JD, Zhang L. Influence of core protein sequence on glycosaminoglycan assembly. *Curr Opin Struct Biol.* 1996; 6:663–670. [PubMed: 8913690]
 37. Heit JA, Petterson TM, Owen WG, Burke JP, De AM, Melton LJ III. Thrombomodulin gene polymorphisms or haplotypes as potential risk factors for venous thromboembolism: a population-based case-control study. *J Thromb Haemost.* 2005; 3:710–717. [PubMed: 15842356]
 38. Auro K, Komulainen K, Alanne M, Silander K, Peltonen L, Perola M, Salomaa V. Thrombomodulin gene polymorphisms and haplotypes and the risk of cardiovascular events: a prospective follow-up study. *Arterioscler Thromb Vasc Biol.* 2006; 26:942–947. [PubMed: 16456088]
 39. Kunz G, Ohlin AK, Adami A, Zoller B, Svensson P, Lane DA. Naturally occurring mutations in the thrombomodulin gene leading to impaired expression and function. *Blood.* 2002; 99:3646–3653. [PubMed: 11986219]
 40. Delvaeye M, Noris M, De VA, Esmon CT, Esmon NL, Ferrell G, Del-Favero J, Plaisance S, Claes B, Lambrechts D, Zoja C, Remuzzi G, Conway EM. Thrombomodulin mutations in atypical hemolytic-uremic syndrome. *N Engl J Med.* 2009; 361:345–357. [PubMed: 19625716]
 41. Stevens JW, Lentz SR. Countervailing effects on atherogenesis and plaque stability: a paradoxical benefit of hypercoagulability? *Circulation.* 2009; 120:722–724. [PubMed: 19687352]
 42. Eitzman DT, Westrick RJ, Shen Y, Bodary PF, Gu S, Manning SL, Dobies SL, Ginsburg D. Homozygosity for factor V Leiden leads to enhanced thrombosis and atherosclerosis in mice. *Circulation.* 2005; 111:1822–1825. [PubMed: 15809370]
 43. Seehaus S, Shahzad K, Kashif M, Vinnikov IA, Schiller M, Wang H, Madhusudhan T, Eckstein V, Bierhaus A, Bea F, Blessing E, Weiler H, Frommhold D, Nawroth PP, Isermann B. Hypercoagulability inhibits monocyte transendothelial migration through protease-activated receptor-1-, phospholipase-Cbeta-, phosphoinositide 3-kinase-, and nitric oxide-dependent signaling in monocytes and promotes plaque stability. *Circulation.* 2009; 120:774–784. [PubMed: 19687358]
 44. Snyder LA, Rudnick KA, Tawadros R, Volk A, Tam SH, Anderson GM, Bugelski PJ, Yang J. Expression of human tissue factor under the control of the mouse tissue factor promoter mediates normal hemostasis in knock-in mice. *J Thromb Haemost.* 2008; 6:306–314. [PubMed: 18005233]

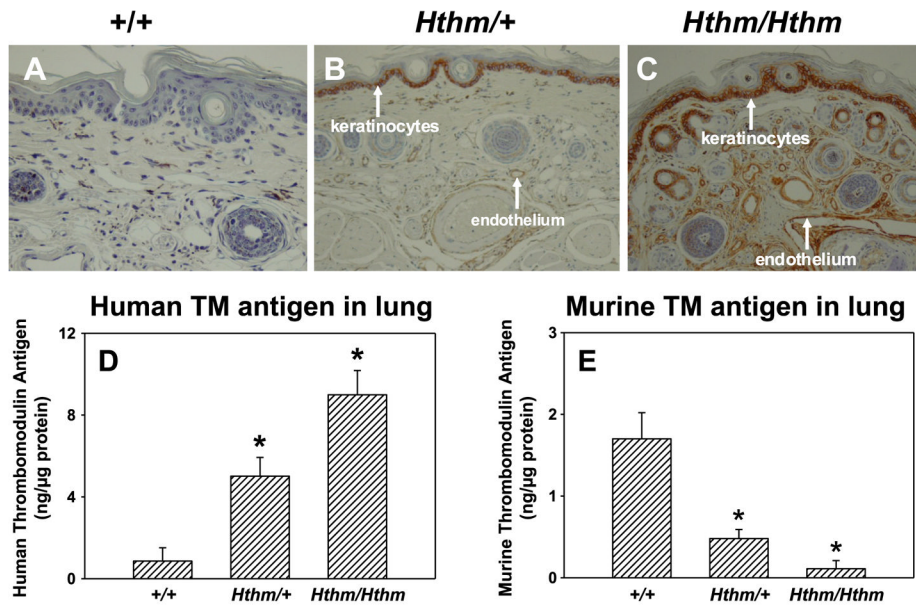


Figure 1.

Expression of human thrombomodulin protein by immunohistochemistry and ELISA. Representative tail sections from +/+ (A), *Hthm/+* (B), or *Hthm/Hthm* (C) mice were stained with anti-human thrombomodulin antibody as described in Methods. Intense staining for human thrombomodulin in endothelium and keratinocytes is demonstrated in *Hthm/Hthm* mice, moderate staining is seen in *Hthm/+* mice, and no specific staining is observed in +/+ mice. Lung lysates of +/+, *Hthm/+*, or *Hthm/Hthm* mice were analyzed for human (D) or murine (E) thrombomodulin antigen by ELISA. Mice were studied at 3 months of age. Values represent mean \pm SE (n = 6 to 20 in each group). *P < 0.05 vs. +/+ mice.

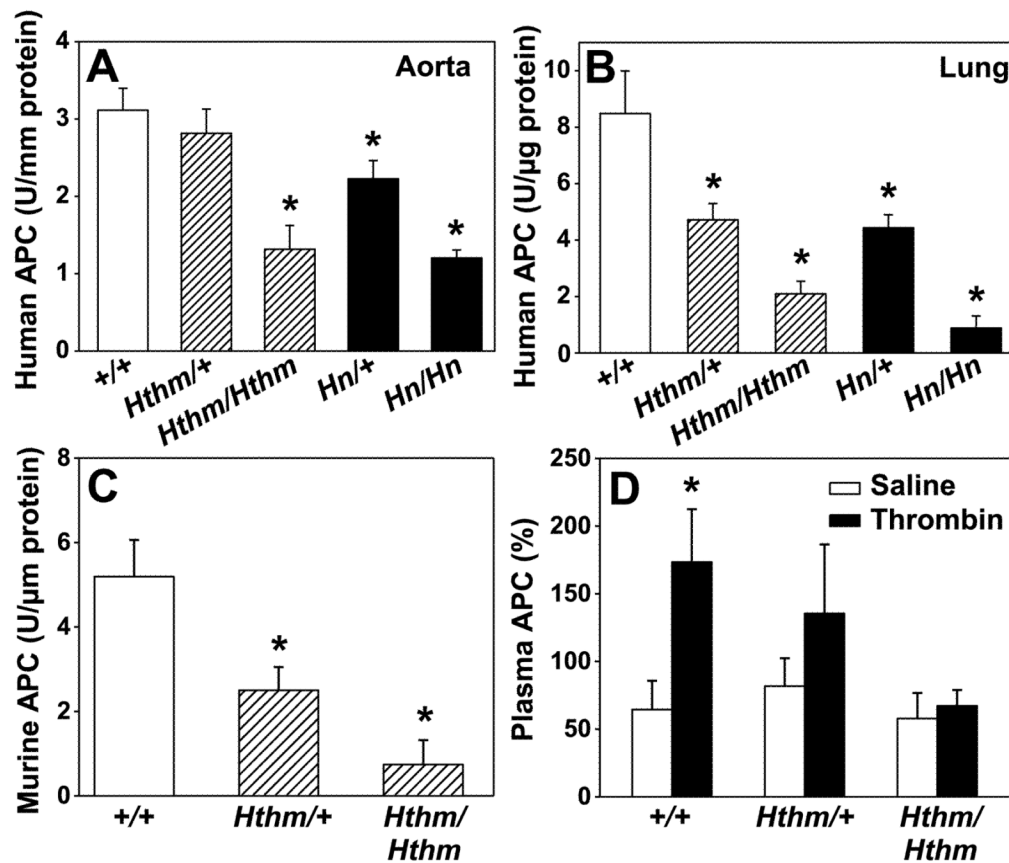


Figure 2.

Protein C activation. Thrombomodulin-dependent activation of protein C was measured in aortic rings (A) or lung lysates (B) of +/+, *Hthm*+, *Hthm/Hthm*, *Hn*+, or *Hn/Hn* mice using 2.6 nM human thrombin and 150 nM human protein C. Mice were studied at 3 months of age. Values represent mean \pm SE (n = 4 for *Hn/Hn* mice; N = 19 to 22 for all other groups). *P < 0.05 vs. +/+ mice. (C) Thrombomodulin-dependent activation of protein C was measured in lung lysates of +/+, *Hthm*+, or *Hthm/Hthm* mice using 2.6 nM murine thrombin and 150 nM murine protein C (n = 3 to 8 in each group). *P < 0.05 vs. +/+ mice. (D) Plasma levels of murine APC were measured following infusion of either saline vehicle or 40 U/kg of human thrombin. Results are reported as percent of APC in pooled normal mouse plasma (n = 5 to 8 in each group). Mice were studied at 3 months of age. Values represent mean \pm SE. *P < 0.05 vs. saline.

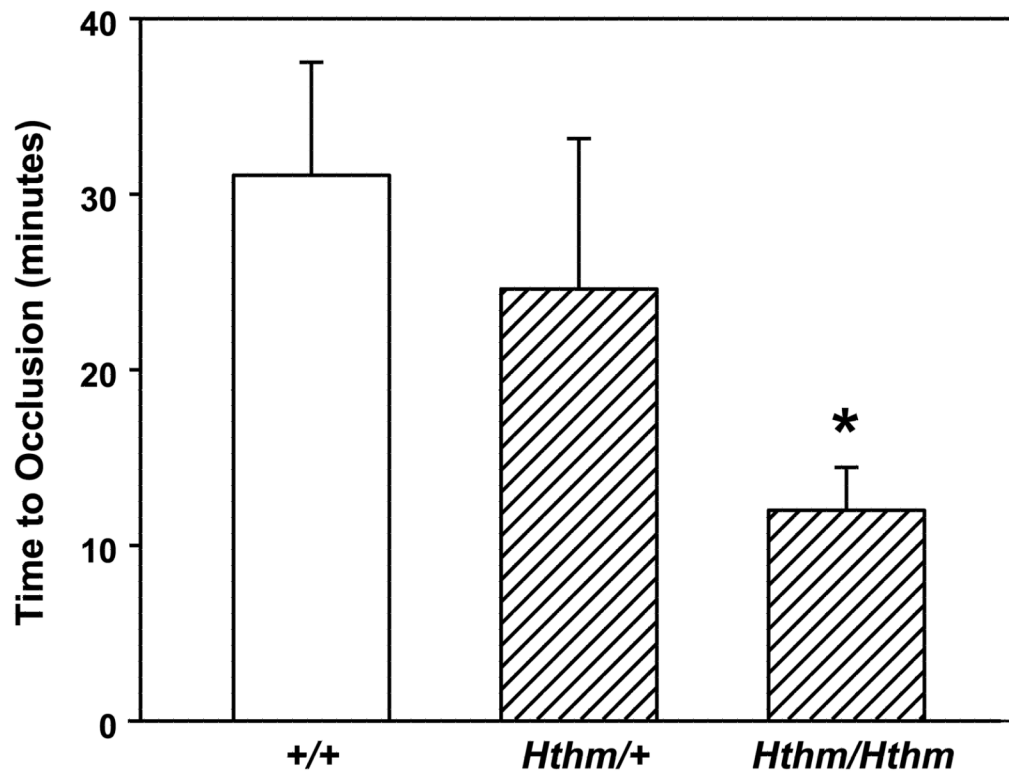


Figure 3. Carotid artery thrombosis following photochemical injury. Susceptibility to thrombosis in +/+, *Hthm*/+, or *Hthm/Hthm* mice was assessed by measuring the time to stable occlusion after photochemical injury of the carotid artery in anesthetized, ventilated mice. Mice were studied at 6 months of age. Thrombosis was induced by injection of 35 to 50 mg/kg of rose bengal. Values represent mean \pm SE (n = 9 to 10 in each group). *P < 0.05 vs. +/+ mice.

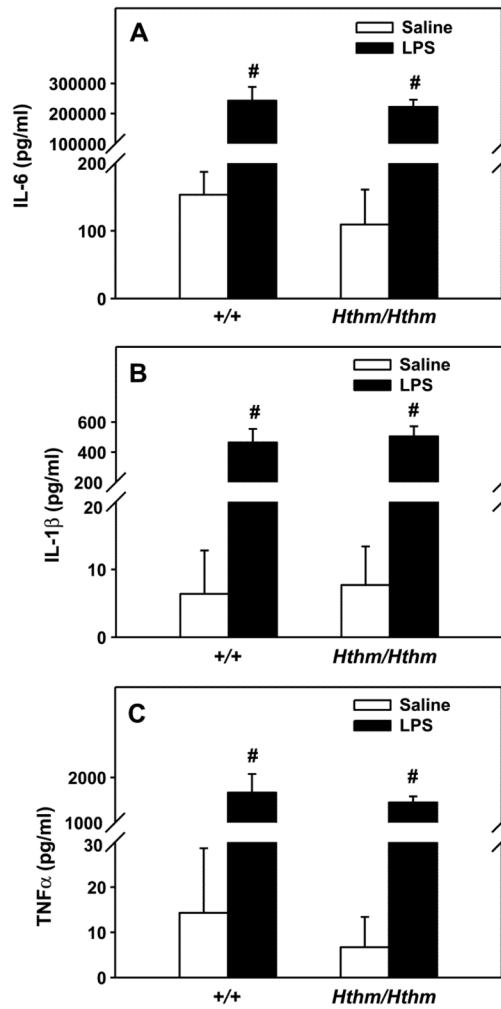


Figure 4.

Response to intraperitoneal injection of endotoxin. Blood samples were obtained 4 hours after intraperitoneal injection of 8 mg/kg LPS or saline vehicle in +/+ and *Hthm/Hthm* mice, and were assayed for serum IL-6 (A), serum IL-1 β (B), and serum TNF α (C). Mice were studied at 12–18 months of age. Values represent mean \pm SE (n = 5 to 13 in each group). # $P < 0.05$ vs. saline.

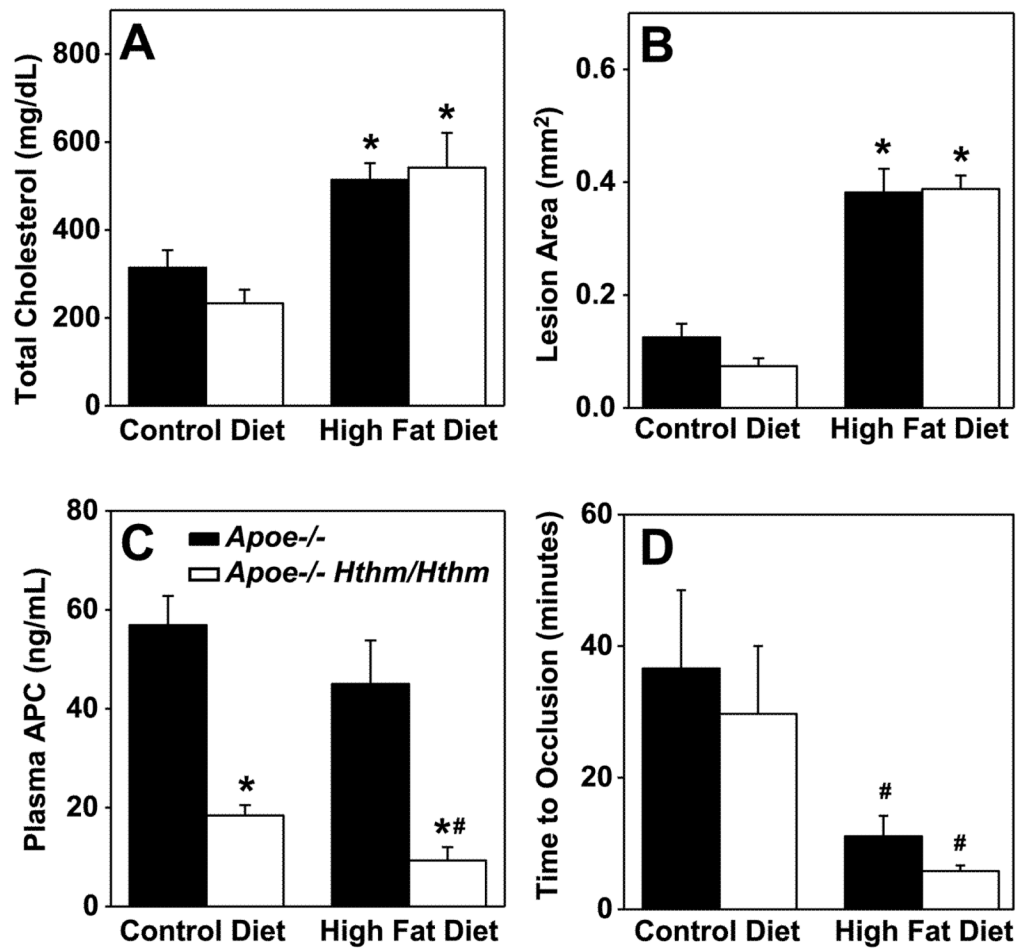


Figure 5.

Phenotype of *Apoe*^{-/-} *Hthm/Hthm* mice. Plasma total cholesterol levels (A), and aortic sinus lesion area (B) in male *Apoe*^{-/-} or *Apoe*^{-/-} *Hthm/Hthm* mice fed either a control diet or a high fat Western diet and studied at 24 weeks of age. (C) Plasma levels of murine APC (reported as ng/mL) following infusion of 40 U/kg of human thrombin. (D) Time to stable occlusion of the carotid artery thrombosis following photochemical injury. Thrombosis was induced by injection of 25 mg/kg of rose bengal. Values represent mean ± SE (n = 6 to 13 in each group). *P < 0.05 vs. control diet; #P < 0.05 vs. *Apoe*^{-/-} mice.

Table 1Quantitative PCR analysis of total (murine + human) thrombomodulin mRNA[†]

	+/+	<i>H^{hm}/H^{hm}</i>	<i>Hⁿ/Hⁿ</i>
Lung	100±19	72±19	76±8
Heart	26±4	20±2	13±2*

[†]The total amount of thrombomodulin mRNA was determined using a probe/primer set that detects regions common to the murine and human transcripts. All mice were on an inbred 129/SvEv background, and were studied at 4–6 months of age. Data are reported as a percentage of the total amount of thrombomodulin mRNA in the lung of +/+ mice. Values represent mean ± SE (n = 4 to 5 in each group).

* P < 0.05 vs. +/+ mice.

Table 2Species-specific quantitative PCR analysis of thrombomodulin mRNA[‡]

	+/+	<i>Hthm</i> /+	<i>Hn</i> /+
Lung			
murine TM mRNA (%)	100±20	43±13*	35±11*
human TM mRNA (%)	0±0	30±6*	26±9*
Heart			
murine TM mRNA (%)	14±2	6±1*	7±2*
human TM mRNA (%)	0±0	15±4*	8±2*
Kidney			
murine TM mRNA (%)	8±1	4±1*	5±1
human TM mRNA (%)	0±0	3±0.4*	4±2*

[‡] Levels of individual murine thrombomodulin and human thrombomodulin transcripts were measured using species-specific real-time PCR primers. All mice were on an inbred 129/SvEv background, and were studied at 4–6 months of age. Data are reported as a percentage of murine thrombomodulin mRNA in the lung of +/+ mice. Values are mean ± SE (n = 4 to 7 in each group).

* P < 0.05 vs. +/+ mice.